MEMS arrays for deformable mirrors

Raji Krishnamoorthy
Thomas Bifano

Boston University, Department of Aerospace and Mechanical Engineering
Boston, Massachusetts 02215

ABSTRACT

A new class of silicon-based deformable mirror for use in optical applications such as adaptive optical systems and optical correlators is being built. The mirror will be a massively parallel system of electrostatically-controlled, interconnected microactuators that can be coordinated to achieve precise actuation and control at a macroscopic level. The deformable mirror system described here will be made up of a planar array of 400 electrostatically actuated actuators, which actuate a laterally continuous mirror at discrete points, resulting in surface-normal deflection of upto 4 μm. Several generations of single actuators as well as arrays of actuators with a mirror sheet over them have been designed, fabricated and tested. Deflection characteristics and pull-in behavior of the actuators have been closely studied. Tests for yield, reliability, resolution and frequency response have given optimistic results. Numerical models of the system have been developed and results from the numerical simulations agree well with experimental results.

KEYWORDS: MEMS, deformable mirror, adaptive optics

2. INTRODUCTION

Some of the significant applications of MEMS technology arise from the ability to organize individual microactuators into arrays which cooperatively perform a macroscopic function. A prominent example of MEMS successfully applied to arrays of interconnected microactuators is the digital projection display[1] based on the digital micromirror device (DMD) built by Texas Instruments. The torsion mirror used in this display is a bistable device, capable of tilting ±10° to reflect incoming light in one of two directions. The DMD technology has also been used in several other applications including coherent optical correlators[2,3], electrophotography printers[4], and as a fiberoptic crossbar switch[5].

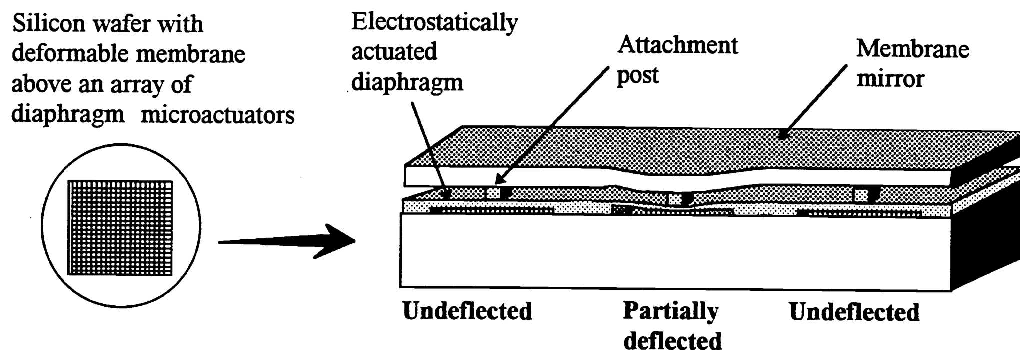

Figure 1: Schematic cross-section of a section of deformable mirror array showing actuator deflection

0-8194-2007-7/95/$6.00

The deformable mirror system described here incorporates a continuous mirror sheet actuated at discrete points, the deformation being normal to the surface and continuous over a desired range. Figure 1 is a schematic showing a cross-section through three actuators in a row with a mirror sheet over them. The actuators are double cantilever beams, a structurally robust design. When voltage is applied between an actuator and the substrate or a ground pad, the electrostatic force developed deflects the actuator toward the substrate. The mirror sheet, which is attached to the actuator at midspan by a post, also deflects as a result, the amount of deflection depending on the applied voltage. In the schematic, the actuator in the center is deflected, while the others are undeflected.

The targeted applications for this MEMS deformable mirror include adaptive optical imaging, projection systems and optical correlators for pattern recognition systems, which are described in the following section. The MEMS deformable mirror has several advantages over the conventional piezoelectrically actuated mirrors. Fabrication is made considerably easier because no discrete assembly is required and the hardware (actuators and mirror) can be integrated on the same chip. It is very inexpensive, with projected costs under $10 for a 400 zone mirror at prototype stage. Since it uses existing semiconductor fabrication technology and can take advantage of batch fabrication processes, the final cost will be much lower. Design changes can be implemented rapidly and inexpensively. Performance is enhanced because the system has a low voltage, low power, reversible operation. It also has increased actuator density allowing higher spatial resolution, is lightweight and can operate at high frequencies. The deformable mirror system can be manufactured as a component of a modular adaptive optics system.

The primary variables to be specified in a deformable mirror system are the number of actuators, the control bandwidth and the maximum actuator stroke. The design goals for the MEMS actuator array system have been determined based on the requirements of a typical adaptive optical imaging system. For astronomical observations, these design parameters can be estimated based on the desired strehl ratio S (which is the ratio of the on-axis intensity of an aberrated image to the on-axis intensity of an unaberrated image), the optical wavelength of interest, the characteristics of the optical disturbance and the optical system aperture, using theoretical turbulence and photonic models. The goal then is to build a deformable mirror device with a 2μm thick membrane mirror over 400 electrostatically actuated diaphragms, optimal actuator size, 8 μm electrostatic gap, 20 nm resolution, 4 μm stroke per actuator, 1 kHz open loop control bandwidth of entire array and 1 cm square active mirror area.

3. APPLICATIONS

Adaptive optical (AO) systems correct aberrations in an optical system through active control of mirror geometry. The most common AO systems use nominally flat, deformable secondary mirrors, whose shape is adjusted to compensate for aberrations in an optical wavefront. One important application of AO is compensation of aberration due to atmospheric turbulence in astronomical telescopes. The process is called phase conjugation, and requires that each of the deformable mirror's many segments or zones is controlled real-time. With AO, the achievable image resolution is greatly enhanced. Currently existing deformable mirrors in AO systems are either segmented mirrors[6], or are continuous mirrors with either continuous membrane piezoelectric bimorph actuators[7] or independent piezoelectric actuators[8]. These systems are typically enormously expensive, heavy and require with an integral cooling system required to eliminate excess heat. By using MEMS technology, the image resolution of an adaptive optical system can be improved while reducing weight, manufacturing time, actuator cost, and assembly complexity.

Optical correlators for pattern recognition perform analog spatial correlation, searching for known spatial patterns within an image. In optical correlators using phase-only filtering, a given image is illuminated by a coherent light source, and is Fourier transformed into spatial frequencies by transmission through a lens, exploiting the properties of Fraunhofer diffraction. A deformable mirror is placed on the focal plane of this lens; the phase information of the Fourier transform of the desired spatial pattern is used to deform this mirror so that the reflected waveform is the product of the Fourier transforms of the image and the pattern. The reflected waveform is passed through a second lens to perform an inverse Fourier transform and is then projected onto a charge-coupled device (CCD) array. The presence of a segment of the image matching the desired spatial pattern will produce a bright spot projected at that location onto the CCD array. The principal commercial application of optical correlators is for pattern recognition, an application of critical importance to the automated manufacturing industry.

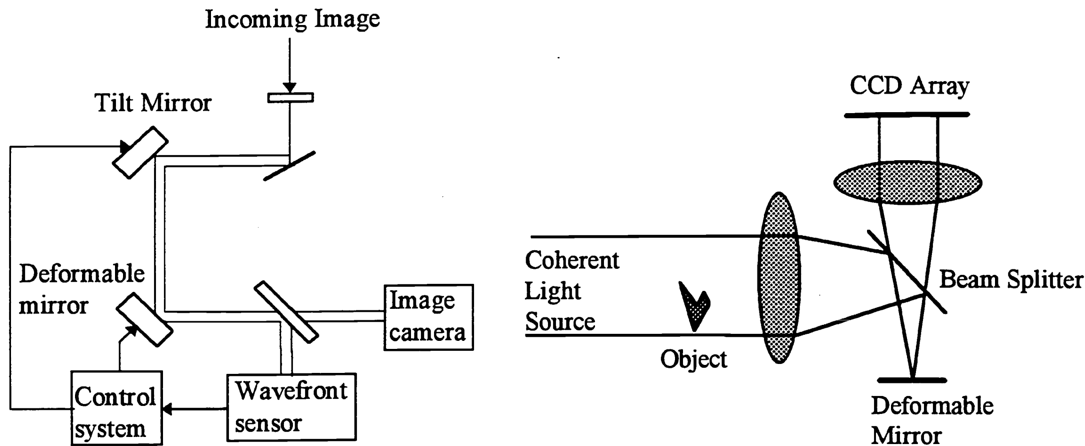

Figure 2: Typical adaptive optical imaging system (left) and optical correlation system (right)

4. FABRICATION

All test devices were fabricated using the ARPA sponsored Multi-User MEMS Process (MUMPs) at the Microelectronics Center of North Carolina. It is a three-layer polysilicon surface micromachining process. Table 1 gives the thickness and description of the various layers in this process.

Table 1: MUMPs layer definitions

LAYER	THICKNESS	PURPOSE
Silicon	100 mm	Substrate
Silicon Nitride	500 nm	Electrical insulation
Polysilicon 0	500 nm	Ground pad
Oxide 1	2 μm	Sacrificial layer
Dimples	750 nm	Avoiding short circuit
Polysilicon 1	2 μm	Structural layer
Oxide 2	0.5 μm	Sacrificial layer
Polysilicon 2	1.5 μm	Structural layer
Metal (Cr-Pt)	0.5 μm	External connection

Figure 3 shows the fabrication sequence for a single actuator with a mirror sheet over it. The substrate was n-type (100) silicon doped with phosphorus. A low stress LPCVD (low pressure chemical vapor deposition) silicon nitride layer was first deposited on substrate to serve as electrical insulation. A low stress LPCVD polysilicon layer (poly 0) was deposited, lithographically patterned and etched in an RIE (Reactive Ion Etch) system to form the ground pads. This was followed by a sacrificial PSG (phosphosilicate glass) layer to electrically isolate this plane from the actuator. The dimples were next transferred to this PSG layer. The dimples correspond to a discontinuity in the poly 0 layer and prevent short circuits by mechanically impeding the diaphragm from contacting the ground pads when fully deflected. This oxide layer was further patterned and etched to form the edge supports for the double cantilevered actuators. A second polysilicon layer (poly 1) which is the first structural layer forming the diaphragm, was deposited. A second sacrificial PSG layer (oxide 2) which was used to separate the mirror sheet from the actuator was then deposited. This oxide was patterned and etched down to poly 1 to form the post. The third polysilicon layer was deposited to form the mirror. Holes were patterened into the top two polysilicon layers to enable subsequent release by wet chemical etch of the sacrificial oxide layers.

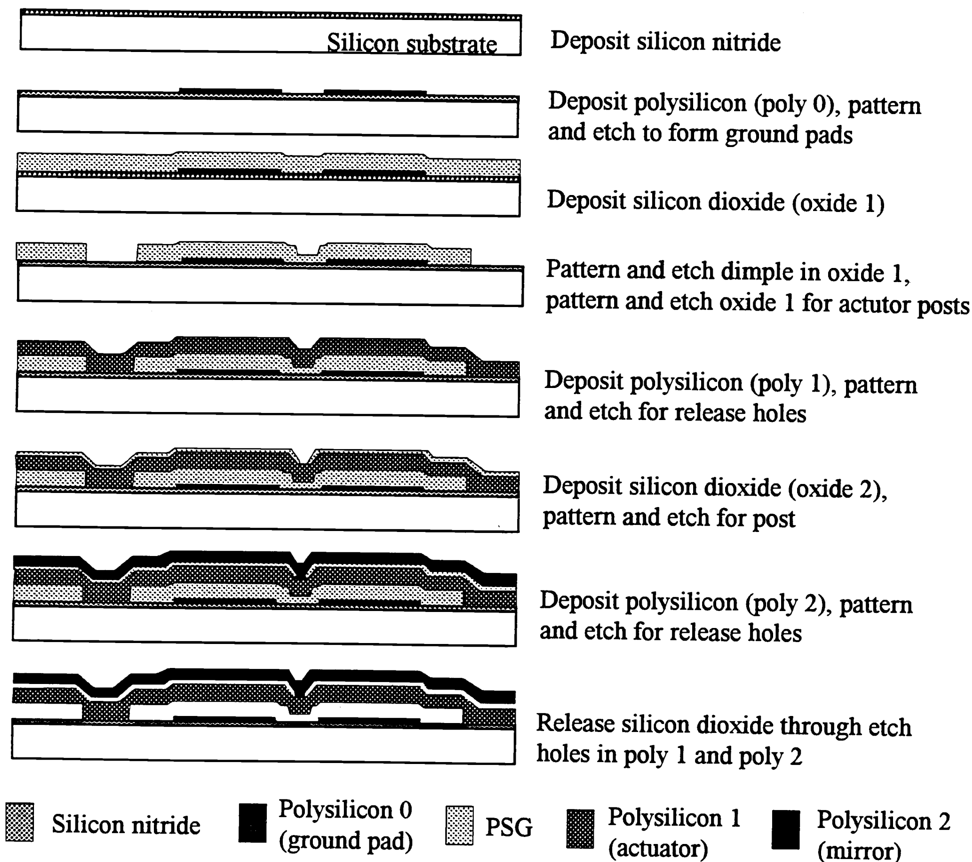

Figure 3: Fabrication sequence for deformable mirror test structures using MUMPs

The next generation of devices and eventually the prototypes will be fabricated in a dedicated process run. Design features for the custom fabrication runs are currently being established.

5. TEST DEVICE DESIGNS

The optimum geometry was selected based on some theoretical and numerical calculations, as well as experimental testing. The best performance to date was obtained with diaphragms that were 350 μm square, 2.0 μm thick, with a 2.0 μm gap. Tests for yield, reliability, frequency response and resolution were conducted using these devices.

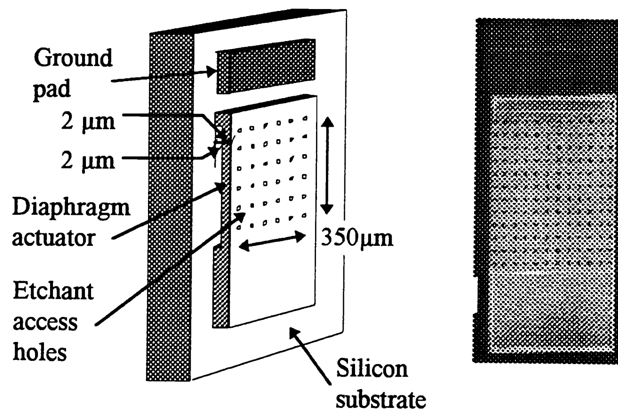

Figure 4: Schematic of an individual actuator, showing optimum dimensions. To the right is an SEM photograph of an actual device.

In a more recent test, a face sheet was included on top of a row of four actuators. The geometry used for all the test structures is a 350 μm square double cantilever, with a 2 μm mirror. Tests are being conducted on both continuous and segmented membrane mirrors. Linear arrays of four as well as planar arrays of nine (schematic shown in Fig. 5) have been fabricated and tested.

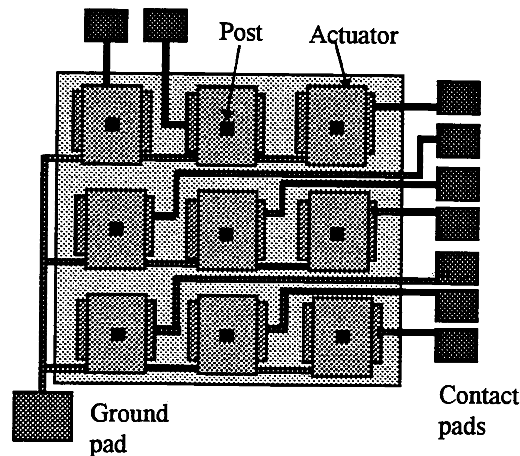

Figure 5: Sketch of a 3x3 array of actuators fabricated as a test structure.

6. PERFORMANCE

To actuate a diaphragm, voltage was applied between the ground pad and the diaphragm using a pair of micro-probes. Deflections were measured using a displacement measuring laser interferometer. This device uses a focused laser beam to measure normal displacement with a position resolution of 0.6 nm and time resolution of 15.6 ns, a range of ±1.3 m, a frequency bandwidth of 0-133 kHz, and a lateral sampling area of several micrometers. In addition, the actuators were visually examined under a Nomarski microscope. Figure 6 shows pictures of a portion of a mirror surface with a single actuator underneath, when the mirror is undeflected and when it has been pulled down.

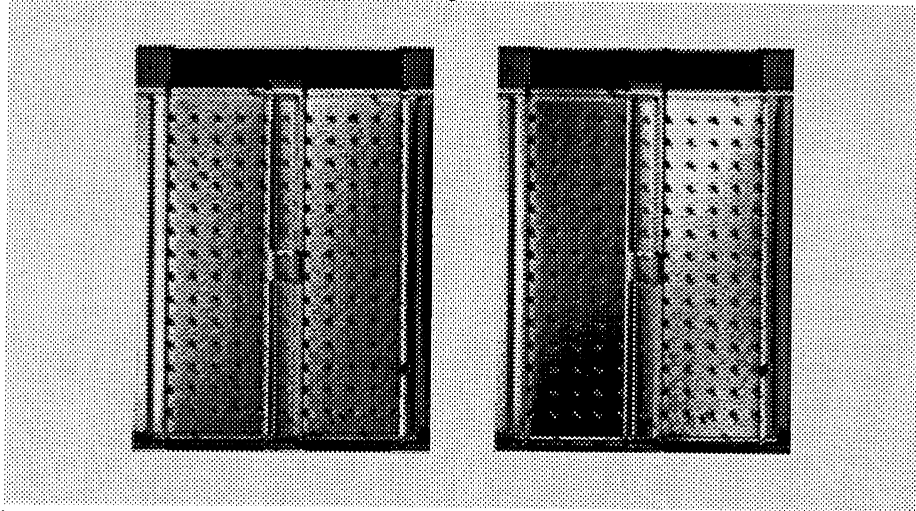

Figure 6: A portion of a mirror with a single actuator underneath viewed under a Normarski microscope at 50X. The mirror is undeflected at 0V (left) and deflected at 100V (right). Visible clearly are the etch holes in the mirror and the attachment post anchoring the mirror to the diaphragm.

Previous MEMS research demonstrated that the average yield for individual actuator designs is 40-60%. Yield and reliability were therefore a major concern, and results from experiments to characterize these have given optimistic results. A total of 487 individual actuators were tested, with a yield of 94.5%. A second concern was frequency response. The actuators were subjected to frequency response tests and were found capable of responding to frequencies of upto 60 kHz. They drew no measurable current, which implies that the array is thermodynamically reversible, as expected for an electrostatic system.

When subjected to a slowly increasing voltage (0-100V), the deflection of the diaphragm increased nonlinearly but quite repeatably until the voltage reached 60V, at which time the diaphragm was deflected by approximately 0.9 μm, shown by the dotted line in Fig. 7. Above this critical voltage, the diaphragm would undergo the well-known electrostatic actuator phenomenon called "snap through instability", instantaneously deflecting all the way to the substrate. When voltage was decreased from the measured critical voltage, the diaphragm remained in its snapped position until the voltage was decreased to 50V, when it decreased nonlinearly following the path along which it had increased. It was found that there was a 10% variability (1σ) in critical voltage among the actuators tested, but less that 0.1% variability in the critical voltage for a given actuator subjected to repeated deflections. This suggests that the actuators in a given array could be used in an open loop actuation control scheme, provided that each actuator's

characteristic critical voltage was previously measured. There was better than 20 nm repeatability in deflection for a given actuator subjected to periodic electrostatic actuation.

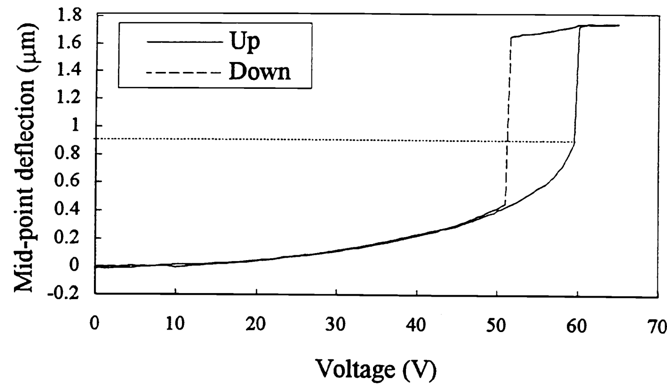

Figure 7: Measured deflection as a function of increasing and decreasing voltage

There was no electrical coupling between actuators. Since devices so far have been fabricated in a multi-user run with pre-defined layer thicknesses, there is insufficient space between the actuator and mirror to achieve the full 4.0 µm deflection. There are points of contraflexure along the mirror surface, making it impossible to study the coupling effects between actuators. These will be studied subsequently following a custom fabrication run.

The deflection was also numerically simulated using a one-dimensional electromechanical model. This is a reasonable approximation since the structure has initially parallel components with a small gap compared to the lateral dimensions[9]. The diaphragm was modeled as a double cantilever beam, with a gap-dependent, electrostatic actuating force. Deflection is a function of applied electric field, material properties, and geometry.

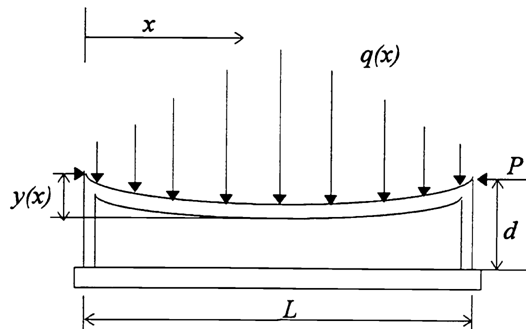

Figure 8: Actuator model for analytical and numerical evaluation

From elasticity theory, the beam deflection $y(x)$, taking into consideration the electrostatic force and residual force is

$$\frac{d^4y(x)}{dx^4}+\frac{P}{EI}\frac{d^2y(x)}{dx^2}=\frac{q(x)}{EI} \tag{1}$$

with the boundary conditions being

$$y(0)=y(L)=0$$
$$y'(0)=y'(L)=0$$

where P is the axial force at the supports, E is the elastic modulus of the beam and I is the moment of inertia of the beam. From electrostatics, the distributed force acting on the beam as a function of position along the beam is

$$q(x)=\frac{\kappa^2\varepsilon_0 w}{2(d-y(x)^2)}V^2 \tag{2}$$

where κ is the dielectric constant of the gap material, ε_o is the permittivity of free space and V is the applied voltage. This gives the fourth order non-linear ordinary differential equation

$$(d-y(x)^2)\frac{d^4y(x)}{dx^4}+(d-y(x)^2)\frac{d^2y(x)}{dx^2}\frac{P}{EI}\frac{d^2y(x)}{dx^2}=\frac{\kappa^2\varepsilon_0 w}{2(d-y(x)^2)}V^2 \tag{3}$$

The solution to this equation for a gap of 2 μm and an approximated residual stress of 10 MPa gave a maximum deflection at the mid-point of 0.87 μm and a critical voltage of 60V. These results based on the numerical model agree notably well with the experimentally measured values of maximum deflection before snapping and the critical voltage at which snap-through occurred. Figure 9 shows the numerically simulated deflection at the mid-point of the beam as a function of voltage.

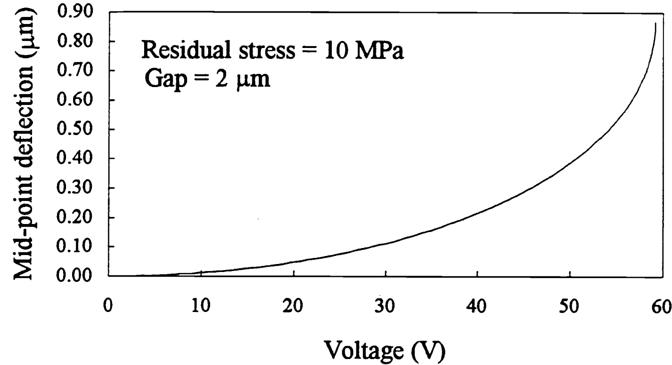

Figure 9: Numerical simulation of actuator deflection

7. ACKNOWLEDGMENTS

This research is currently being funded by a three-year contract with ARPA, and was initiated on a Small Grant for Exploratory Research from the National Science Foundation (# DDM9317937). We are grateful to the staff at the Microelectronics Center of North Carolina for their generous assistance. Thanks to Nelsimar Vandelli, Adam Maines and Laura Rennie, who have contributed to different aspects of this project.

8. REFERENCES

1. J.M. Younse, "Mirrors on a chip," IEEE Spectrum, pp. 27-31, November 1993.

2. D.A. Gregory, R,D. Juday, J. Sampson, R. Gale, R.W. Cohn, S.E. Monroe, "Optical characteristics of a deformable-mirror spatial light modulator," *Optical Letters*, Vol. 13, no. 10, 1988.

3. J.M. Florence, R.O. Gale, "Coherent optical correlator using a deformable mirror device spatial light modulator in the Fourier plane," *Applied Optics*, Vol. 27, no. 11, p. 2091, 1988.

4. E. Nelson, L. Hornbeck, "Micromechanical spatial light modulator for electrophotography printers," *Proceedings of SPSE, Fourth International Congress on Advances in Non-Impact Printing Technologies*, p. 427, 1988.

5. G. McDonald, M. Boysel, J. Sampsell, "4x4 fiberoptic crossbar switch using the deformable mirror device," *Technical Digest on Spatial Light Modulators and Applications*, Optical Society of America, Vol. 14, pp. 80-83, 1990.

6. B. Hulburd, D. Sandler, *Optical Engineering*, Vol. 29, no. 10, 1990.

7. E. Steinhaus, S.G. Lipson, *J. Opt. Soc. Am.*, Vol. 69, no. 3, 1979.

8. M.A. Ealey, J. F. Washeba, *Optical Engineering*, Vol. 29, no. 10, 1990.

9. P. Osterberg, H. Yie, X. Cai, J. White, S. Senturia, "Self-consistent simulation and modeling of electrostatically deformed diaphragms," *Proc. MEMS 1994* (Osio, Japan), pp. 28-32, 1994.